Swirl Effect on the Flame Propagation at Idle in a Spark Ignition Engine

Shin Hyuk Joo, Kwang Min Chun*
Department of Mechanical Engineering, University of Yonsei
Younggy Shin
Department of Mechanical Engineering, University of Sejong

The objectives of the study are to investigate the effect of swirl on the flame propagation and to propose a flame propagation model that predicts the behavior of the flame front in the presence of significant swirl flow field by analyzing flame images pictured with a high speed digital video at idle. The velocity distribution of the charge in the cylinder was measured using an LDV measurement system. From the experimental results and analyses, a new flame propagation model is proposed in which flame frontal locations can be traced by superposing the convective flow field and the uniform expansion speed of the burned gas, and the proposed model reveals that the increase of the flame propagation speed in the presence of swirl motion within 1 ms after ignition is mainly due to the flame stretch, and mainly due to increased turbulence intensity later than 1 ms after ignition.

Key Words : Flame Propagation, Swirl, S.I. Engine, Idling

Nomenclature

SI	: Spark ignition
SOHC	: Single overhead cam
MPFI	: Multi port fuel injection
BTDC	: Before top dead center
ATDC	: After top dead center
LDV	: Laser doppler velocimetery
MID	: Mixture injection device
BSA	: Burst spectrum analyzer
FFT	: Fast fourier transform
v_c	: Convective velocity
u_b	: Burned gas expansion velocity
v_f	: Flame front velocity
B	: Bore
m	: Mass
r	: Radius
v	: Velocity
C_f	: Friction factor
λ	: Empirical constant
μ	: Dynamic viscosity
Re	: Reynolds number
A_s	: Flame silhouette area
L_s	: Flame silhouette perimeter
u_f	: Flame expansion speed
S_b	: Flame burning speed
S_L	: Laminar burning velocity speed
$\tilde{x}_b$	: Residual gas fraction
x_b	: Mass fraction burned
Γ	: Angular momentum
ω_s	: Equivalent solid-body angular velocity
R_s	: Swirl ratio
ρ	: Density
τ	: Wall shear stress
ϕ	: Fuel/air equivalence ratio
T_0	: Temperature of standard state
T_u	: Temperature of unburned mixture
P	: Pressure
P_0	: Pressure of standard state

* Corresponding Author,
E-mail : icelab1@yonsei.ac.kr
TEL : +82-2-361-2819 ; **FAX** : +82-2-312-2159
Address : Department of Mechanical Engineering Yonsei University Shinchon-dong 134 Seodaemoon-gu Seoul 120-749 Korea. (Manuscript **Received** August 16, 1999; **Revised** March 16, 2000)

1. Introduction

In general, there are substantial cylinder pressure variations on a cycle-by-cycle basis in a spark ignition engine, particularly at idle (Heywood, 1988). It is well known that the cycle-by-cycle variations decrease as the flame propagation speed increases (Young, 1980, 1981). Large number of researches were carried out to increase the flame propagation speed and one of plausible methods is to strengthen the in-cylinder flow turbulence. To clarify the interaction between in-cylinder flow and flame propagation process, several techniques such as pressure measurement, ion probe, optical fiber, and high speed photography have been used. Among these techniques, high speed photography has been a useful tool for many researchers in understanding how in-cylinder flow affects combustion process in a S. I. engine (Arcoumanis, 1990, 1993, Checkel, 1993, Joo, 1999). For example, Gatowski et al. (Gatowski, 1985) reported the behavior of the flame propagation analyzed from the images taken in a square cross-section piston visualization engine. They also developed a flame propagation model to estimate the mean expansion speed of the burned gas and the flame front area under the assumption that the flame propagates spherically if there exists no significant swirl in the flow. Due to various limitations, however, the model can not be extended to the flow field with significant swirl. In order to overcome the limitations, Shen et al. (Shen, 1994) proposed a flame propagation model based on the assumption that an elliptic flame front is formed in the high swirl flow field during the flame development and that the shape is maintained throughout the rest of the combustion process. However, high-speed photography revealed that the geometry of the flame front evolves quite differently from that at the early flame development. Therefore, further study is required to understand interactions of the flame front shape and the flow field. The purpose of this study is to propose a plausible flame propagation model that predicts the behavior of the flame front in the presence of significant swirl flow field by analyzing flame images obtained with a high speed digital video.

2. Experimental Apparatus

Figure 1 shows a schematic of the experimental apparatus used in the study. The experimental transparent engine was modified from a 4 cylinder, 4 stroke, SOHC, MPFI production engine. The displacement volume of one cylinder, compression ratio, bore, stroke, and the diameter of the quartz window on piston top were 374.5cc, 8.6, 76.5mm, 81.5mm, 52mm, respectively. Since the purpose of the experiment is to investigate the effect of high swirl on the flame propagation behavior, a special mixture supply system was adopted (Joo, 1999). Stoichiometric amounts of fuel and air are metered by a conventional fuel injector and a solenoid valve, respectively. The mixture is driven into the cylinder by the pressure difference between the atmosphere and the cylinder. The intake manifold is blocked so that the mixture is fed only from the supply system. To intensify swirl in the combustion chamber, the mixture is guided in the circumferential direction of the intake valve by a tube with I.D. of 4 mm at the exit of the supply system. For high-speed photography, a visualization window made of quartz was mounted on the piston top and flame images were reflected at the 45(tilted aluminum-

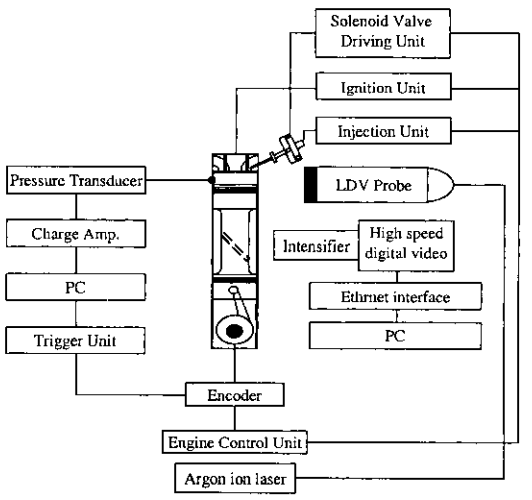

Fig. 1 Experimental setup

coated mirror and presented to the high speed digital video with an image intensifier. Resolution and maximum capture rate of the high speed digital video were 512×384 photosensitive pixels and 2000 fps (frames per second), respectively. To obtain velocity distribution of the flow field in the combustion chamber, side walls of the chamber were replaced with quartz windows for visual access to the combustion chamber for an LDV measurement system.

3. Experimental Method

3.1 High speed photography

The flame propagation process was pictured at the speed of 2,000 frames/sec. The engine operating condition was at 800 rpm, 0.8 bar of IMEP (indicated mean effective pressure), 10° BTDC of ignition timing, and 14.6 of air-to-fuel ratio. Since the flame luminescence was too weak for flame images to be taken with the high speed digital video itself, due to the nature of premixed combustion in a S. I. engine, an image intensifier was added to the camera to get enhanced images.

3.2 Measurement of velocity distribution in the combustion chamber

The LDV system consisted of a 5W Ar-ion laser and BAS data analysis equipment of DANTEK Co. The measurement of velocity distribution was conducted for the engine motoring at the same operating condition as the engine firing case.

4. Flame Propagation Model

As mentioned in the introduction, a new flame propagation model is required to explain the behavior of the flame propagation in the presence of a strong swirl flow field. From the experimental results, a new model is proposed based on the following assumptions.

(1) Turbulence intensity of the unburned mixture ahead of the flame is spatially uniform: This assumption has been validated by many studies such as the spherical flame propagation model (Heywood, 1988, Stone, 1996, Ma, 1996, Blizard, 1974, Tabaczynski, 1980) and cycle-resolved turbulence measurement results (Witze, 1985, Hall, 1986).

(2) The mean expansion speed of the flame front is proportional to turbulence intensity: Since the observation that the burning speed of the mixture is proportional to turbulence intensity is well accepted (Groff, 1980), and the assumption is plausible in the same context.

(3) The flame front is convected by the flow: Since the convective flow field equally affects the burned gas and the unburned mixture, the flame front will be displaced to new positions dictated by the flow field. Any gradient in the convective flow field will stretch the flame front. This assumption along with the assumption of the spatially uniform turbulence intensity will determine the final geometry of the flame front. The validity of the assumption will be discussed in the following section in conjunction with the experimental results.

(4) Angular momentum of the charge is conserved during the combustion process: Since the angular momentum loss due to the friction on the cylinder walls is relatively small, as will be discussed in the following section, the tangential velocity distribution in the radial direction is kept constant during the combustion process; this will provide the information on the convective flow field.

Based on the above assumptions, the following flame propagation model is proposed. Linear superposition of the convective velocity and the uniform expansion speed of the burned gas allows identification of the new flame frontal location when the time step associated with the geometric evolution of the flame front is small enough. By the nature of nonlinear governing equations involved in the combustion process, it is not possible theoretically to do such linear superposition. However, when the time step is small enough, linear approximation could be appropriate for the sake of engineering analysis. The linear approximation was employed to predict the flame frontal locations with the proposed flame propagation model and the results showed good agreement with the locations experimentally observed.

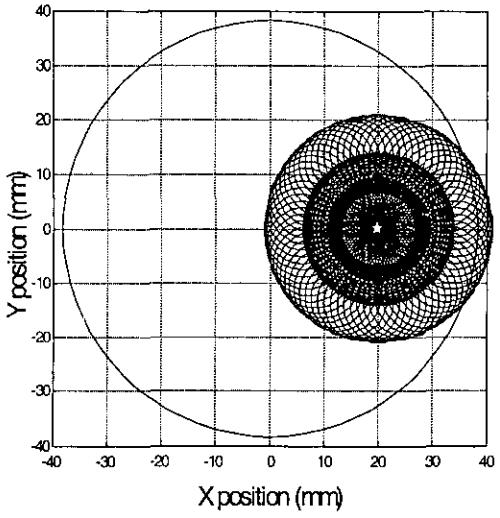

Fig. 2 An example of flame propagation calculated using a proposed flame propagation model for the case of no swirl

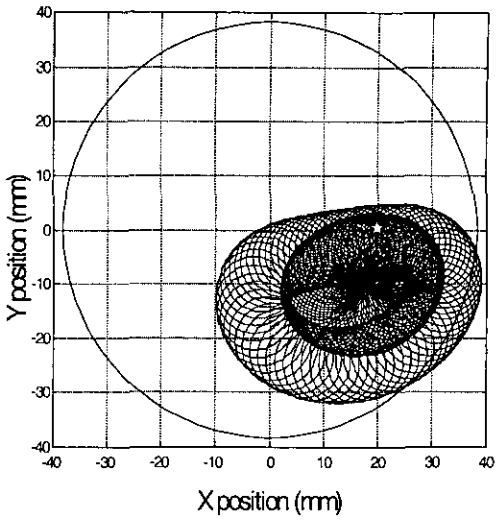

Fig. 3 An example of flame propagation calculated using a proposed flame propagation model for the case of swirl

Linear superposition of the convective velocity and the expansion speed of the burned gas can be expressed mathematically as Eq. (1).

$$v_c + u_b = v_f \tag{1}$$

where v_c, u_b, v_f represent the convective velocity, the burned gas expansion velocity, and the flame velocity respectively.

Figure 2 shows the propagation of the flame front with no swirl depicted by the flame propagation model. The flame kernel developed at the point (20,0) propagates in infinite number of circles centered on the flame front at the current time step with the radius determined by the expansion speed of the burned gas. The locus of outer intersection of the circles forms the new flame front corresponding to the next time step. The complete flame propagation can be described by finding the loci at successive time sequences. In the model, the principle of the flame propagation is quite similar to that of wave propagation, and it is assumed that the expansion speed of the burned gas is spatially uniform. This leads to spherical expansion of the flame front at the characteristic expansion speed mainly determined by turbulence intensity.

Figure 3 shows a calculated result of the propagation of the flame front with swirl as depicted by the flame propagation model. It can be observed that the flame front is stretched by the convective flow field. The flame kernel developed at the point (20, 0) propagates in a fashion implying that the flame front is displaced by the convective flow field and then it expands uniformly at the displaced frontal location. The final flame front due to the uniform expansion is found by the locus of outer intersections of infinite number of circles centered on the displaced frontal location and with the radius that is the product of the flame expansion and the time interval between two consecutive flame fronts.

5. Test Results and Discussion

5.1 High-speed flame pictures

Figure 4 shows the behavior of the flame front that develops at the spark plug and expands while being displaced by the convective flow. All legends are representing the time after the start of ignition. Flame pictures were taken using a high speed digital video with an image intensifier. The flame fronts were extracted from the pictures using a commercial graphic program, Photoshop, and they were overlaid in one graph with their locations digitized by a program written in C. It is observed that the flame fronts move fast in the

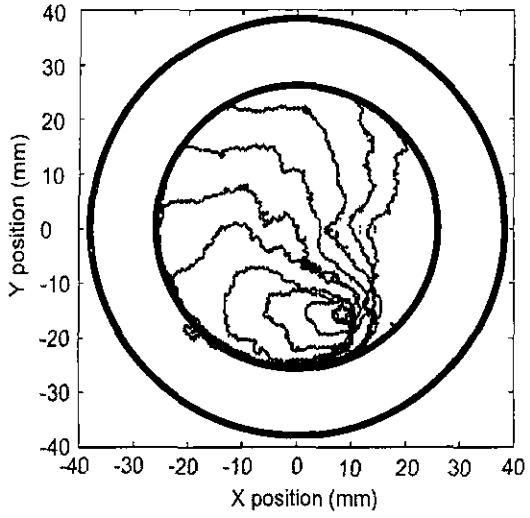

Fig. 4 Flame propagation for a cycle for the case of swirl measured using a high speed digital video

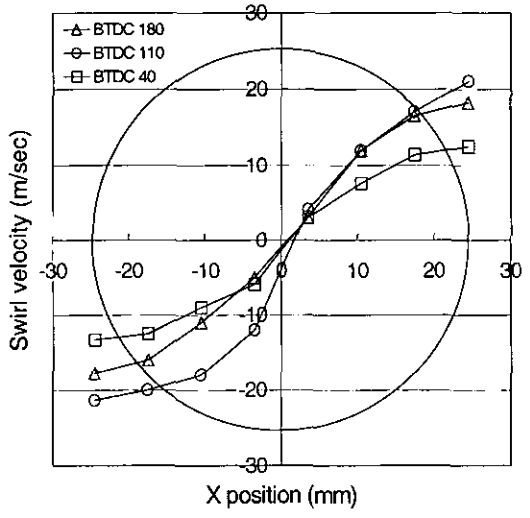

Fig. 5 Velocity profile for the case of swirl during compression process measured using an LDV

swirl direction whereas they do slowly in the opposite direction. This is because the expanded flame front is displaced by the convective flow field.

5.2 Measurement of convective flow field in the combustion chamber

Figure 5 shows the results of flow measurement at 180°, 110°, 40° BTDC during compression. The flow measurements were made at the positions of

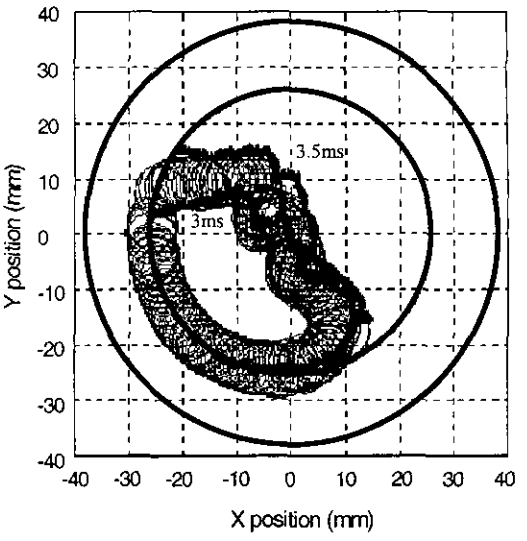

Fig. 6 Prediction of the flame shape using a flame propagation model and comparison with the measured flame shape (3msec after the start of ignition)

every increment of 7 mm in X direction from the axis of the cylinder in the plane 5 mm below the top deck of the cylinder. The flow measurement after 40° BTDC crank angles was not possible because the piston blocked the optical access through the window. According to Fig. 5, it is observed that the velocity profiles are approximately axisymmetric and similar in shape although their maximum values are different. Thus, they can be collapsed into a single curve by normalizing each profile with its maximum value. The empirical similarity provides valuable information regarding the convective flow field during the combustion in conjunction with the conservation of angular momentum.

5.3 Estimation of the expansion speed of the burned gas and the swirl flow fieldr

Figure 6 shows the comparison of the measured flame frontal locations and the estimated one by the proposed flame front model for two consecutive frames pictured at 3ms and 3.5ms after the start of ignition. In estimating the flame frontal location, the unknown variables are the flame expansion speed and the scale factor which will convert the normalized tangential velocity distri-

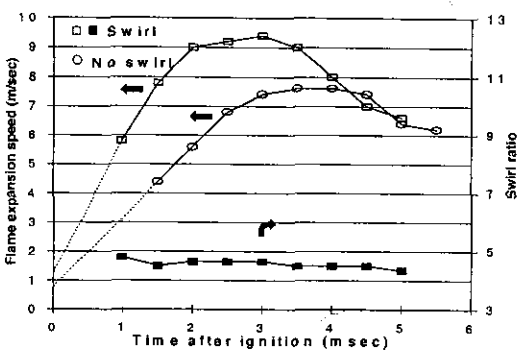

Fig. 7 Calculated flame expansion speed and swirl ratio determined from flame images

bution into real velocities. The scale factor corresponds to the tangential velocity at the rim of the visualization window whose diameter is 52 mm. The two variables were determined by comparing the measured and estimated flame fronts. In the figure, the inner circle is the boundary of the window and the outer one is that of the piston. The thick solid traces represent the flame fronts pictured in two consecutive frames with the interval of 0.5 ms. To plot the estimated flame frontal locations, the flame front pictured at the previous time step is displaced by the distance swept at the convection velocity during 0.5 ms at corresponding locations. At that time, the flame front is stretched by the convective velocity gradients in the radial direction. At the displaced location, many number of circles are drawn and their radius is found by curve-fitting the outer intersections of the circles with the pictured flame front. The curve-fitting procedure was repeated for every frame of pictures during the combustion and the scale factors for the convective flow field and the flame expansion speed were estimated from the procedure. Although the estimated flame front couldn't predict local flame distortions, it is observed that they are in good agreement on average.

Figure 7 shows the results of the estimated flame expansion speeds and swirl ratio calculated from scale factors and normalized velocity distribution. The swirl ratio during combustion is nearly constant as was assumed. The expansion speed could be obtained from the moment of 1.0 or 1.5 msec after ignition because the flame luminescence before that was too weak to be captured. It is observed that the expansion speed with swirl is larger than that without swirl, showing 25% increase in its maximum value. In both cases, the expansion speed increases in the beginning and approaches to a maximum in the middle, finally decreasing at the final stage. Such behavior of the expansion speed coincides with the observations of other studies (Berreta, 1983) obtained from the flame propagation model of spherical expansion with no swirl. From the result, it is confirmed that the general behavior of the expansion speed known for the flame front model of spherical expansion is also observed in the proposed flame front model. The observation of nearly constant swirl ratio during the combustion and the effects of the swirl on increased flame expansion speed in Fig. 7 can be confirmed analytically as follows:

5.4 Conservation of angular momentum

Along with the normalized velocity profile, the conservation of angular momentum provides the information on the convective flow field during combustion. To prove its conservation during combustion, the angular momentum and the angular momentum loss due to friction on the walls were estimated. For the estimation, a pancake type combustion chamber was assumed. Since the displacement of the piston during the combustion period of 5.5 ms is small, any change in the volume of the combustion chamber was neglected. To calculate the shear stresses on the cylinder head and the piston top, the in-cylinder flow was modeled as the flow between two flat plates under fully developed flow condition.

The angular momentum in the combustion chamber can be expressed as Eq. (2)

$$\Gamma = \int_0^{B/2} r \times m(r) \times v(r)\, dr \tag{2}$$

where Γ is the angular momentum and B, r, m, v are bore, radial distance from the cylinder center, mass and velocity respectively.

The angular momentum in the combustion chamber can also be expressed using an equivalent solid-body angular velocity ω_s:

$$\Gamma = \int_0^{B/2} r^2 \times m(r) \times \omega_s dr \tag{3}$$

From Eq. (2) and Eq. (3) an equivalent solid-body angular velocity was found and the swirl ratio which is defined as Eq. (4) was calculated.

$$R_s=\frac{\omega_s}{2\pi N} \tag{4}$$

There is friction on the cylinder wall, cylinder head, and piston crown. This friction can be estimated with sufficient accuracy using friction formulas developed for flow over a flat plate, with suitable definition of characteristic length and velocity scales (Heywood, 1988). Friction on the cylinder wall can be estimated from the wall shear stress τ:

$$\tau=\frac{1}{2}\rho\left(\frac{\omega_s B}{2}\right)^2 C_f \tag{5}$$

where ω_s is the equivalent solid-body swirl. The Friction factor C_f is given by the flat plate formula:

$$C_f=0.037\lambda(\mathrm{Re}_B)^{-0.2} \tag{6}$$

where λ is an empirical constant introduced to allow for differences between the flat plate and cylinder wall ($\lambda\approx1.5$) and Re_B is the equivalent of the flat plate Reynolds number:

$$\mathrm{Re}_B=\frac{\rho(B\omega_s/2)(\pi B)}{\mu} \tag{7}$$

Friction on the cylinder head and piston crown can be estimated from expressions similar to Eq. (5). However, since the tangential velocity v_θ at the wall varies with radius, the shear stress should be evaluated at each radius and integrated over the surface:

$$\tau(r)=C_1\frac{1}{2}\rho[v_\theta(r)]^2\mathrm{Re}^{-0.2} \tag{8}$$

$$\text{with } \mathrm{Re}=\frac{\rho v_\theta(r)\,r}{\mu} \tag{9}$$

where C_1 is an empirical constant (≈0.055).

The estimated results are angular momentum: 2.9344×10^{-5} (kgm^2/sec), equivalent solid-body angular velocity: 381.83 (rad/sec), swirl ratio: 4.56, angular momentum loss during combustion: 6.9656×10^{-7} (kgm^2/sec), fraction of the angular momentum loss: 2.37 (%) respectively. This small amount of angular momentum loss is in good agreement with the experimental result.

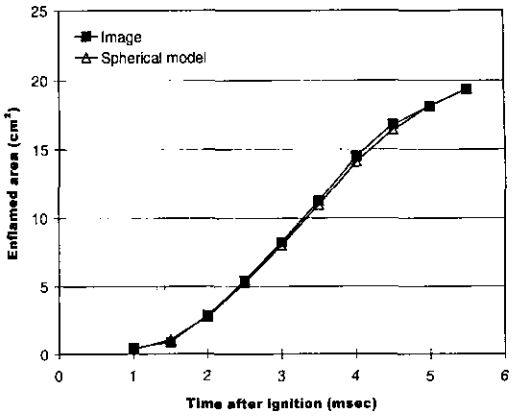

Fig. 8 Comparison of the enflamed areas between measured and calculated using a spherical model

5.5 The effect of swirl on the turbulence intensity and the flame stretch

Any increase of the flame propagation speed in the presence of the swirl flow field is considered to be due to enhanced turbulence intensity and flame stretch. The flame propagation speed is proportional to the rate of change of the enflamed area. The rate of change of the enflamed area A_s (area in pictured flame images) is proportional to the perimeter and the expansion speed of the burned gas as shown in the relationship below. (Heywood, 1988)

$$\frac{dA_s}{dt}=L_s\times u_f \tag{10}$$

Here, the flame image perimeter L_s represents flame stretch and the expansion speed u_f is proportional to turbulence intensity. The effect of the flame stretch on the increase of the enflamed area can be investigated by comparing the enflamed area obtained from the images by counting the enflamed pixels, with the one calculated from the conventional flame propagation model of spherical expansion. Figure 8 shows the comparison of the enflamed areas. The enflamed area by the conventional model was calculated by assuming that the gas expands spherically from the spark plug with the expansion speed obtained from the flame images in the presence of swirl using the proposed model. Figure 8 indicates that both enflamed areas are nearly the same, suggesting

that the flame stretch caused by the convective velocity gradient in the radial direction later than 1 ms after ignition contributes little to the increase of the flame frontal area. In other words, the increase of the flame propagation speed in the presence of swirl motion later than 1 ms after ignition is mainly due to the increased turbulence intensity rather than the flame stretch.

When it comes to the combustion period of 1 msec after ignition, clear flame images couldn't be acquired due to strong luminescence of ignition spark, but the flame expansion speed at the start of ignition can be calculated analytically under the assumption of spherical expansion of the flame front as follows (Heywood, 1988):

As the expansion speed of the burned gas and the flame expansion speed are almost the same, the flame expansion speed u_f can be expressed as Eq. (11)

$$\frac{u_f}{S_b}=\frac{\rho_u/\rho_b}{[(\rho_u/\rho_b)-1]x_b+1} \tag{11}$$

Where S_b is the flame burning speed and x_b is the mass fraction burned.

At the start of ignition, the flame burning speed S_b can be assumed to be the same with laminar burning speed S_L. S_L can be expressed as Eq. (12)

$$S_L=S_{L,0}\left(\frac{T_u}{T_0}\right)^{\alpha}\left(\frac{P}{P_0}\right)^{\beta} \tag{12}$$

where $T_0=298$K, $p_0=1$ atm and $S_{L,0}$, α, β are empirical constants which can be represented by

$$\alpha=2.18-0.8(\phi-1) \tag{13}$$

$$\beta=-0.61+0.22(\phi-1) \tag{14}$$

$$S_{L,0}=B_m+B_\phi(\phi-\phi_m)^2 \tag{15}$$

For gasoline, the parameters ϕ_m, B_m, B_ϕ are 1.21, 30.5, −54.9, respectively. (Rhodes, 1985)

Burned gas in the unburned cylinder charge due to residual gases causes a substantial reduction in the laminar burning velocity, and the laminar burning velocity at any burned gas mole fraction ($\tilde{x}_b$) can be expressed as Eq. (16).

$$S_L(\tilde{x}_b)=S_L(\tilde{x}_b=0)(1-2.06\tilde{x}_b^{0.77}) \tag{16}$$

In this study the burned gas mole fraction was assumed to be 25% (Toba, 1976)

The initial flame expansion speed was also estimated by extrapolation to time 0 as shown in Fig. 7. Calculation result is $u_f=0.81$ m/sec and extrapolation results are $u_f=0.80$ m/sec without swirl, $u_f=1.30$ m/sec with swirl, respectively.

The expansion speed calculated from the analytical relationship under the assumption of spherical expansion of the flame front above is in good agreement with that obtained by extrapolation from the flame images with no swirl, but it is less than that with swirl. At the start of ignition, $S_b\approx S_L$, $x_b=0$, $\rho_u/\rho_b\approx 4$, and these lead to $u_f\approx 4\times S_L$ in Eq. (11). This means that there is little effect of the turbulence intensity on the flame expansion speed in the initial stage. Therefore, the reason why the expansion speed estimated from flame images with swirl is larger than that of calculation is not from the increased turbulence intensity, but from the initial flame stretch. In conclusion, the reason why the swirl flow increases the flame propagation speed at the initial point (within 1 msec after ignition) is mainly due to the flame stretch.

6. Conclusions

High -speed flame pictures were taken from a spark ignition engine with a visualization window on top of the piston operated at idle. To investigate the effect of swirl on the flame propagation, a special mixture supply system was used and the velocity distribution in the combustion chamber was measured using an LDV measurement system. From the experimental results and analysis, the following conclusions were obtained:

(1) When there exists significant swirl in the flow, the tangential velocity distributions at different crank angles can be approximated into a single normalized curve.

(2) The proposed flame propagation model in which the flame front is displaced by the distance (the convective velocity times the time interval) and then expands uniformly outwards at the flame expansion speed that is proportional to turbulence intensity is found to be a good approximation to explain the behavior of pictured flame fronts.

(3) The expansion speed obtained from the

proposed flame propagation model in the presence of significant swirl shows a similar trend to the expansion speed with no swirl that increases in the beginning of combustion, approaches a maximum in the middle and decreases towards the end.

(4) The proposed model reveals that the increase of the flame propagation speed in the presence of swirl motion within 1 ms after ignition is mainly due to the flame stretch, and mainly due to increased turbulence intensity later than 1 ms after ignition.

References

Berreta, G. P., Rashidi, M. and Keck, J. C., 1983, "Turbulent Flame Propagation and Combustion in Spark Ignition Engines," *Combustion and Flame*, 52:217~245.

Blizard, N. S. and Keck, J. C., 1974, "Experimental and Theoretical Investigation of Turbulent Burning Model for Internal combustion Engines," *SAE Technical Paper* 740191.

Arcoumanis, C., Hu, Z., Vafidis, C. and Whitelaw, J. H., 1990, "Tumbling A Mechanism for Turbulence Enhancement in spark-ignition Engines," *SAE Technical Paper* 900060.

Arcoumanis, C. and Bae, C-S., 1993, "Visualization of Flow/Flame Interaction in a Constant Volume Combustion Chamber," *SAE Technical Paper* 930868.

Stone, C. R., Brown, A. G. and Beckwith, P., 1996, "Cycle-by-Cycle Variations in Spark Ignition Engine Combustion," *SAE Technical Paper* 960613.

Groff, E. G. and Maketunas, F. A., 1980, "The Nature of Turbulent Flame Propagation in a Homogeneous Spark-ignited Engine," *SAE Technical Paper* 800133.

Ma, Fanhua, Shen, Huixian, Liu, Chuanli, Wu, Deyu, Li, Guowei and Jiang, Deming, 1996, "The Importance of Turbulence and Initial Flame Kernel Center Position on the Cyclic Combustion Variations for Spark-ignition Engines," *SAE Technical Paper* 961969.

Shen. H., Hinze, P. C., John Heywood, B., 1994, "A Model for Flame Initiation and Early Development in SI Engine and Its Application to Cycle-to-Cycle Variations," *SAE Technical Paper* 942049.

Hall, M. J., Bracco, F. V., and Santavicca, D. A., 1986, "Cycle-Resolved Velocity and Turbulence Measurements in an IC Engine with Combustion," *SAE Technical Paper* 860032.

Gatowski, Jan A. and Heywood, John B., 1985, "Effects of valve-shrouding and Squish on Combustion in a Spark-Ignition Engine," *SAE Technical Paper* 852093.

Heywood, John B., 1988, *Internal Combustion Engine Fundamentals*, Mc-Grow Hill, pp. 413~423, 406~410.

Checkel, M. David, and Ting, David Sing-Khing, 1993, "Turbulence Effects on Developing Turbulence Flames in a Constant Volume Combustion Chamber," *SAE Technical Paper* 930867.

Rhodes, D. B. and Keck, J. C., 1985, "Laminar Burning Speed Measurements of Indolene-Air-Dilnent Mixtures at High pressure and Temperature," *SAE Technical Paper* 850047.

Joo, S. H. Chun, K. M., 1999, "Improvement of the SI Engine Idle combustion Stability using a Fuel-Air Mixture Injection Device," *JSAE Paper*, 9932566.

Tabaczynski, R. J., Trinker, F. H. and Shannon, B. A. S., 1980, *Combustion and Flame* 39: 111-121.

Toba, T., Nohira, H. and Kobashi, K., 1976, "Evaluation of Burned Gas Ratio (BGR) as a Predominant Factor to NOx," *SAE Technical Paper* 760765.

Witze, P. O., and Mendes-Lopes, J. M. C., 1985, "Direct Measurement of the Turbulent Burning Velocity in a Homogeneous-Charge Engine," *SAE Technical Paper* 851531.

Young, M. B., 1980, "Cyclic Dispersion-Some Quantitative Cause and Effect Relationships," *SAE Technical Paper* 800459.

Young, M. B., 1981, "Cyclic Dispersion in the Homogeneous-charge spark-ignition Engine-A Literature Survey," *SAE Technical Paper* 810020.